Immunity
Article

The Shaping of T Cell Receptor Recognition by Self-Tolerance

Stephanie Gras,[1] Scott R. Burrows,[2] Lars Kjer-Nielsen,[3] Craig S. Clements,[1] Yu Chih Liu,[1] Lucy C. Sullivan,[3] Melissa J. Bell,[2] Andrew G. Brooks,[3] Anthony W. Purcell,[4] James McCluskey,[3,5,*] and Jamie Rossjohn[1,5,*]
[1]The Protein Crystallography Unit, Department of Biochemistry and Molecular Biology, Monash University, Clayton, Victoria 3800, Australia
[2]Cellular Immunology Laboratory, Queensland Institute of Medical Research, Brisbane 4029, Australia
[3]Department of Microbiology and Immunology, University of Melbourne, Parkville, Victoria 3010, Australia
[4]Department of Biochemistry and Molecular Biology and Bio21 Molecular Science and Biotechnology Institute, University of Melbourne, Parkville, Victoria 3010, Australia
[5]These authors contributed equally to this work
*Correspondence: jamesm1@unimelb.edu.au (J.M.), jamie.rossjohn@med.monash.edu.au (J.R.)
DOI 10.1016/j.immuni.2008.11.011

SUMMARY

During selection of the T cell repertoire, the immune system navigates the subtle distinction between self-restriction and self-tolerance, yet how this is achieved is unclear. Here we describe how self-tolerance toward a trans-HLA (human leukocyte antigen) allotype shapes T cell receptor (TCR) recognition of an Epstein-Barr virus (EBV) determinant (FLRGRAYGL). The recognition of HLA-B8-FLRGRAYGL by two archetypal TCRs was compared. One was a publicly selected TCR, LC13, that is alloreactive with HLA-B44; the other, CF34, lacks HLA-B44 reactivity because it arises when HLA-B44 is coinherited in *trans* with HLA-B8. Whereas the alloreactive LC13 TCR docked at the C terminus of HLA-B8-FLRGRAYGL, the CF34 TCR docked at the N terminus of HLA-B8-FLRGRAYGL, which coincided with a polymorphic region between HLA-B8 and HLA-B44. The markedly contrasting footprints of the LC13 and CF34 TCRs provided a portrait of how self-tolerance shapes the specificity of TCRs selected into the immune repertoire.

INTRODUCTION

$CD8^+$ T cells expressing αβ T cell receptors (TCRs) recognize peptides bound to major histocompatibility complex class I (pMHC-I) molecules. Importantly, T cells are restricted such that they recognize processed peptides only when they are presented by self-MHC molecules (Zinkernagel and Doherty, 1974). To ensure protective immunity against pathogens encountered by the human population, the human leukocyte antigen (HLA) locus has evolved into the most polymorphic region in the human genome (Marsh et al., 2005). This polymorphism not only enhances breadth of ligand binding in outbred populations but also fundamentally shapes the specificity and size of the host TCR repertoire, which is matured during thymic development (Messaoudi et al., 2002). Thus, despite mechanisms with potential to generate 10^{15} different TCRs in humans, positive and negative T cell selection culls the repertoire to approximately 10^8 such TCRs, the diversity of which is required for effective protective immunity (Arstila et al., 1999). During this selection process, the T cell repertoire must navigate the fine distinction between self-restriction and self-tolerance, including tolerance to all host HLA molecules (Hogquist et al., 1993; Jameson et al., 1995). Precisely how the HLA genotype of heterozygous individuals influences the structural specificity of the responding T cell repertoire has not been visualized at the point of the TCR-pMHC interaction.

As a consequence of thymic selection, TCRs are inherently cross-reactive, and studies have revealed how TCRs can mold around a given pMHC-I landscape (and vice versa) (Garcia et al., 1998; Godfrey et al., 2008; Reiser et al., 2003; Rudolph et al., 2006). Moreover, structural studies of the TCR-pMHC complex have provided an understanding of the versatility of this interaction and include examples of antiviral, antitumor, autoreactive and alloreactive TCR-pMHC complexes (Archbold et al., 2008; Clements et al., 2006; Deng and Mariuzza, 2007; Godfrey et al., 2008). Previously, it has been established how different TCRs can recognize the same pMHC (Dai et al., 2008; Ding et al., 1998; Feng et al., 2007), thereby providing insight into defined interaction motifs as well as the versatility of the T cell repertoire. The variability in the observed TCR docking modes is presumably a reflection of the polymorphic nature of the HLA as well as the intrinsic variability of the TCR. Nevertheless, the TCR and pMHC maintain a rough docking mode, in which the Vα domain and Vβ domains are positioned over the α2-helix and the α1-helix respectively (Godfrey et al., 2008). Interestingly, the few autoimmune TCRs that have been solved to date exhibit atypical binding modes in comparison to "antimicrobial" TCR-pMHC complexes (Hahn et al., 2005; Li et al., 2005), in that the former tend to focus toward the N-terminal region of the peptide, whereas the latter are generally focused more toward the middle or C-terminal end (Deng and Mariuzza, 2007; Nicholson et al., 2005). Moreover, the interactions that the autoreactive TCRs make with the anitgen (Ag) appear suboptimal, which correlates with the need for these autoreactive TCRs to escape negative selection (Deng and Mariuzza, 2007; Nicholson et al., 2005). Whether these unusual docking modes are restricted to autoreactive TCRs or also arise in the pathogen-driven, self-tolerant repertoire is unclear.

Despite the constraints of MHC restriction, a surprising number of mature T cells can recognize "non-self" MHC molecules and

are termed alloreactive. The structural basis of such alloreactivity is presently limited to one murine system (Archbold et al., 2008). Specifically, the well-studied 2C TCR adopted two different docking strategies in recognizing self and non-self MHC molecules, even though there were considerable similarities in the self and non-self pMHC surfaces (Colf et al., 2007; Rossjohn and McCluskey, 2007).

Previously, we have explored the in vivo memory cytotoxic T lymphocyte (CTL) response to an immunodominant HLA-B8-restricted epitope, FLRGRAYGL, from the latent EBV antigen, EBNA 3A (Burrows et al., 1990). Remarkably, the immune response to HLA-B8-FLRGRAYGL is characterized by type III-biased TCR usage (the reproducible selection of clonal TCR sequences) identifiable in unrelated HLA-B8$^+$ individuals (Burrows et al., 1990; Gras et al., 2008; Kjer-Nielsen et al., 2002a; Turner et al., 2006). We have characterized the structural and biophysical basis for this biased TCR usage, whereby the LC13 TCR focused upon the P7^{Tyr} residue of the peptide and the C-terminal end of the HLA-B8 Ag-binding cleft (Borg et al., 2005; Kjer-Nielsen et al., 2002b; Kjer-Nielsen et al., 2003). Conservative substitutions at positions P7^{Tyr} or P8^{Gly} of the peptide virtually abrogated recognition by the LC13 TCR, thereby highlighting the specificity of this interaction. Nevertheless, the public LC13 TCR displays alloreactivity toward certain HLA-B44 allotypes (B*4402 and B*4405) (Burrows et al., 1994; Burrows et al., 1995). Notably, in neither HLA-B8/B*4402 nor B8/B*4403 heterozygotes is the public LC13 CTL clonotype detected in the mature T cell repertoire (Burrows et al., 1997a; Burrows et al., 1995), presumably as a result of negative selection of these T cells. However, a vigorous HLA-B8-restricted CTL response toward FLRGRAYGL persists in these individuals, albeit at a slightly lower precursor frequency (Burrows et al., 1995). Interestingly, these CTLs from HLA-B8$^+$B44$^+$ individuals now express different T cell receptor gene combinations, and the fine specificity of the response generally shifts toward either the P1^{Phe} or the P8^{Gly} residue of FLRGRAYGL, and there is concomitant loss of B44 reactivity (Burrows et al., 1994; Burrows et al., 1995). This indicates that the T cell repertoire contains considerable redundancy in receptors with appropriate specificity for HLA-B8-FLRGRAYGL, providing an opportunity to directly examine the structural bases of repertoire selection dictated by trans-HLA allotypes. The CF34 CTL clone (*TRAV14*01*, *TRBV11-2*03*) represents one such dominant clonotype of the TCRs in HLA-B8$^+$B44$^+$ individuals whose T cells exhibit exquisite sensitivity to substitutions at P1^{Phe} and are tolerant of their endogenous B44 allotype (Burrows et al., 1994; Burrows et al., 1995).

Here we structurally compare how the TCRs from the archetypal LC13 and CF34 anti-viral CTLs interact with the same HLA-B8-restricted, Ag-specific (FLRGRAYGL) complex. The LC13 TCR is immunodominant in HLA-B8$^+$ individuals yet alloreactive toward HLA-B44, and consequently, LC13 TCR is deleted from the repertoire in HLA-B8$^+$B44$^+$ individuals. CF34 arises in the context of HLA-B44 as a trans-HLA allele (i.e., it is present in HLA-B8$^+$B44$^+$ individuals) and therefore is nonreactive with HLA-B44. The observed shift in the pMHC footprint between these two TCRs provides a compelling picture of how the requirement for self-tolerance shapes the specificity of the antiviral T cell repertoire. Namely, the CF34 TCR shifts its footprint to a site of polymorphism between HLA-B8 and HLA-B44, and in doing so "sees" the differences between these HLA molecules, thereby providing a basis for the avoidance of autoreactivity.

RESULTS

Contrasting Specificities for the Viral Determinant

In EBV-infected HLA-B8$^+$B44$^+$ individuals, the HLA-B44 alloreactive, public LC13 CTL clone is no longer selected from the T cell repertoire and is replaced instead by an oligoclonal T cell repertoire, also directed against the HLA-B8-FLRGRAYGL determinant but now lacking reactivity with the B44 allotype (Burrows et al., 1995). Within this oligoclonal population, the CF34 TCR (*TRAV14*01-TRAJ49*, *TRBV11-2*03-TRBD2*01-TRBJ2-3*) exhibited heightened specificity toward the P1^{Phe} position in CTL killing assays but was insensitive to mutations at the P8^{Gly} position (Burrows et al., 1995). In contrast, the public LC13 TCR from HLA-B8$^+$B44$^-$ individuals was sensitive to amino acid substitutions at the P8^{Gly} position but not at the P1^{Phe} position (Kjer-Nielsen et al., 2003). Flow-cytometric analysis with HLA-B8 tetramers that incorporated analogs of the FLRGRAYGL epitope with P1^{Phe} and P8^{Gly} substitutions (TLRGRAYGL and FLRGRAYVL, respectively) confirmed the contrasting specificities of the LC13 and CF34 CTL clones (Figures 1A and 1B). To better understand the structural basis for this shift in specificity, the CF34 TCR was expressed, refolded, and purified, allowing comparison to the LC13 TCR. The recombinant CF34 TCR was functionally intact; it reacted with conformationally specific anti-TCR monoclonal antibodies (mAbs), and moreover native gel-shift analysis demonstrated that the CF34 TCR could ligate to the HLA-B8-FLRGRAYGL complex yet did not bind to an irrelevant pMHC epitope (data not shown). By surface plasmon resonance (SPR) analysis, the affinity (Kd) of the CF34 TCR for HLA-B8-FLRGRAYGL was determined to be 8.9 μM, which compared favorably to a Kd of 15 μM for the LC13 TCR- HLA-B8-FLRGRAYGL interaction (Borg et al., 2005; Ely et al., 2006; Ely et al., 2005) (Figure 1C, Table S1). The association constant (K_{on}) and dissociation constant (K_{off}) for the LC13 TCR was 30,950 $M^{-1}\cdot s^{-1}$ and 0.56 s^{-1}, respectively, which was in agreement with previous studies (Borg et al., 2005). The CF34 TCR interacted with the HLA-B8-FLRGRAYGL complex with a slower K_{on} of 7,630 $M^{-1}\cdot s^{-1}$ and a longer K_{off} of 0.18 s^{-1} (calculated from Figure 1C).

Next we compared the sensitivity of the CF34 TCR and the LC13 TCR to substitutions at positions P1^{Phe}, P7^{Tyr}, and P8^{Gly} within the FLRGRAYGL peptide (P1^{Thr}, P1^{Tyr}, P7^{Phe}, and P8^{Val}) bound to HLA-B8. Both the LC13 and CF34 TCRs exhibited the same high degree of specificity toward the P7^{Tyr} residue; they showed an 88% and 94% reduction, respectively, in affinity with HLA-B8^{FLRGRAFGL} in comparison to interaction with the cognate HLA-B8-FLRGRAYGL (Figures 1C and 1D; also Table S1). The LC13 TCR was sensitive to substitution at P8^{Gly}; it was virtually unable to bind to HLA-B8-FLRGRAYVL (Kd > 200 μM; Figure 1D). Alternatively, the affinity of the CF34 TCR for B8-FLRGRAYVL remained comparable to that of the cognate interaction. In contrast to this pattern, the affinity of the LC13 TCR for P1^{Phe} mutations was essentially the same as for the cognate interaction (Figure 1D; also Table S1), whereas CF34 was particularly sensitive to the substitutions at P1^{Phe} and

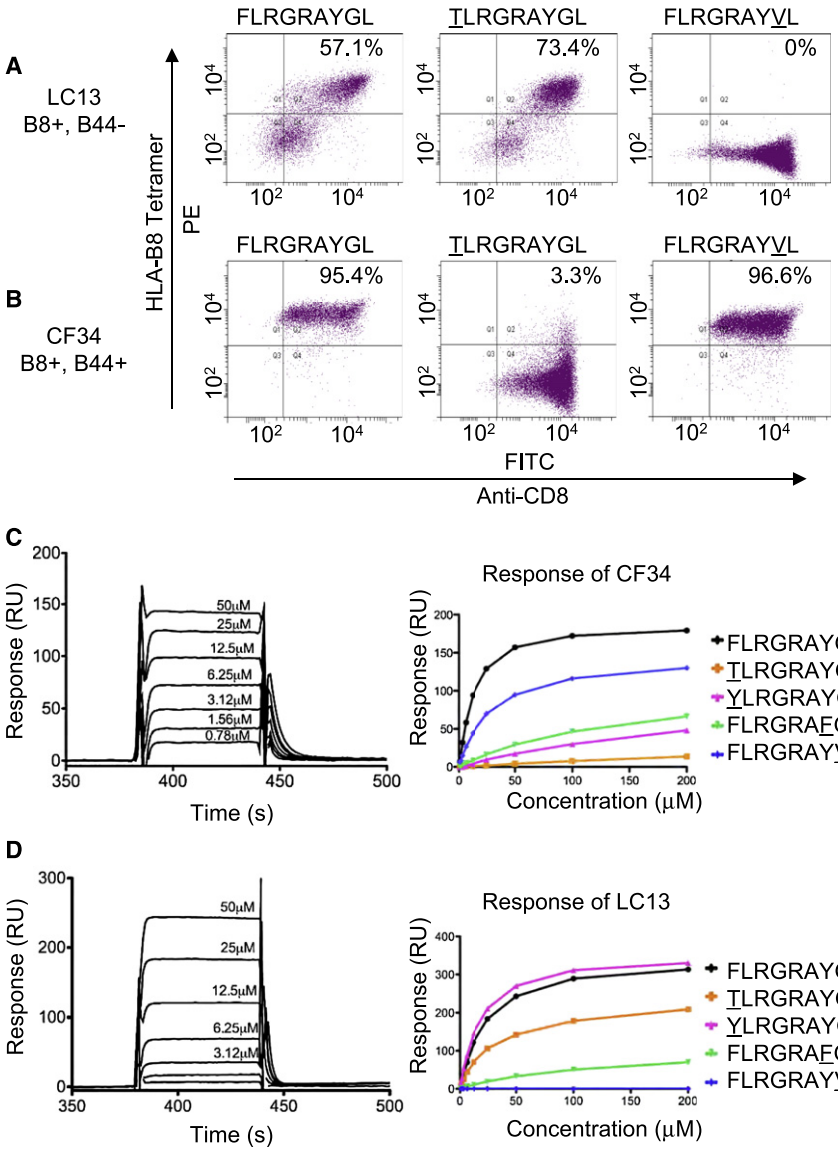

Figure 1. Specificities of the CF34 TCR and LC13 TCRs

HLA-B8 tetramer staining of LC13 (A) and CF34 (B) cytotoxic T lymphocyte clones with differing amino acid substitutions (underlined) in the FLRGRAYGL epitope. Numbers in the top right quadrant indicate the percentage of cells costaining with the CD8 antibody and each of the three different tetramers. This staining pattern was observed in two individual experiments. Shown is surface plasmon resonance analysis of graded concentrations of refolded CF34 (C) and LC13 TCR (D) binding to HLA-B8-FLRGRAYGL containing substitutions in the FLRGRAYGL peptide (underlined). Binding curved for the wild-type peptide FLRGRAYGL (in black) and variants of the peptide, F1→T in orange, F1→Y in pink, Y7→F in green, and G8→V in blue are shown. The biacore experiments were conducted minimally in duplicate.

exhibited markedly reduced affinity (>200 μM) for both HLA-B8-$^{\underline{Y}LRGRAYGL}$ and HLA-B8-$\underline{T}$LRGRAYGL (Figure 1C; also Table S1). Taken together, these results indicate that although the LC13 TCR was focused on the C-terminal P7^{Tyr}, the CF34 TCR exhibited heightened specificity toward the N terminus of the FLRGRAYGL epitope.

Overview of the CF34 TCR-HLA-B8-FLRGRAYGL Complex

Given the markedly different specificities of the CF34 and LC13 TCRs toward HLA-B8-FLRGRAYGL, we hypothesized that the CF34 TCR would adopt a quite different footprint to engage the HLA-B8-FLRGRAYGL complex in comparison to the previously solved LC13 TCR (Kjer-Nielsen et al., 2003). To examine this, we purified the CF34 TCR-HLA-B8-FLRGRAYGL complex and solved the structure at 2.80 Å resolution to an R_{fac} and R_{free} of 22.2% and 27.0%, respectively (see Table 1 and Figures 2A–2D). The initial experimental phases clearly showed unbiased electron density for the FLRGRAYGL peptide (data not shown), and moreover, the electron density at the CF34 TCR-HLA-B8-FLRGRAYGL interface was unambiguous.

The CF34 TCR docked at approximately 58° across the long axis of the HLA-B8-FLRGRAYGL binding cleft (Figures 2A and 2C); this docking angle falls within the range of TCR-pMHC complexes determined to date (Rudolph et al., 2006) and is similar to the 60° docking angle of the LC13 TCR-HLA-B8-FLRGRAYGL interaction (Kjer-Nielsen et al., 2003) (Figure 2D). However, the CF34 TCR was located over the N terminus of the HLA-B8 Ag-binding cleft, which contrasted the C-terminal docking of the LC13 TCR on HLA-B8-FLRGRAYGL (compare Figures 2C and 2D). Although the CF34 TCR was N-terminally focused, the CF34 TCR still interacted with positions 65, 69, and 155 of the HLA-B8, which is consistent with the observation that TCRs invariably interact with these three positions on pMHC-I (and equivalent pMHC-II) in all TCR-pMHC structures determined to date (Rudolph et al., 2006; Tynan et al., 2005). The total buried surface area (BSA) at the CF34 TCR-HLA-B8-FLRGRAYGL interface was approximately 2180 Å^2, which was similar to the BSA of the LC13 TCR footprint (~2020 Å^2). Moreover, the shape complementarity between the CF34 TCR- and LC13 TCR- HLA-B8-FLRGRAYGL interfaces were 0.65 and 0.61, respectively (Lawrence and Colman, 1993). Consequently, CF34 formed many interactions with HLA-B8-FLRGRAYGL (Table 2), making a total of 127 van der Waals (vdw) interactions, 12 H bonds, and no salt bridges, which compared to 135 vdw interactions, 14 H bonds, and one salt bridge in the LC13 TCR-HLA-B8-FLRGRAYGL complex.

Accordingly, the CF34 adopted a markedly shifted N-terminal footprint on HLA-B8-FLRGRAYLGL in comparison to the

Table 1. Data-Collection and Refinement Statistics

Data-Collection Statistics	CF34-HLA-B8-FLRGRAYGL
Temperature	100K
Space group	*I222*
Cell Dimensions (a, b, c) (Å)	111.56, 171.80, 272.69
Resolution (Å)	72.00-2.80 (2.95-2.80)
Total number of observations	474068 (69644)
Number of unique observations	64663 (9311)
Multiplicity	7.3 (7.9)
Data completeness (%)	99.9 (100)
I/σ_I	7.9 (1.5)
R_{pim} [a] (%)	12.6 (41.7)
Refinement Statistics	
Non-hydrogen atoms	
Protein	13494
Water	4
Resolution (Å)	15.00-2.80
R_{factor} [b] (%)	22.2
R_{free} [b] (%)	27.0
Rms deviations from ideality	
Bond lengths (Å)	0.009
Bond angles (°)	1.258
Ramachandran plot (%)	
Most-Favored Region	85.5
Allowed Region	11.8
Generously allowed region	2.3

Values in parentheses are for the highest-resolution shell.
[a] $R_{pim} = \Sigma_h [1/(N-1)]^{1/2} \Sigma_i |I_i(h) - < I(h) >| \Sigma_h \Sigma_i I_i(h)$, where I is the observed intensity and $< I >$ is the average intensity of multiple observations from symmetry-related reflections.
[b] $R_{factor} = \Sigma_{hkl} || F_o | - | F_c || / \Sigma_{hkl} | F_o |$ for all data except approximately 5%, which were used for R_{free} calculation.

C-terminal footprint of the LC13 TCR. Nevertheless, despite these differences in footprints, the CF34 TCR engaged the HLA B8-FLRGRAYGL as effectively as the LC13 TCR.

Comparison of the Footprints

Like the immunodominant LC13 TCR, the CF34-like TCRs found in HLA-B8$^+$, B44$^+$ EBV$^+$ donors show strong Vβ bias in that the same β chain is observed in a number of CTL clones from unrelated individuals (Burrows et al., 1995). Moreover, the sequences corresponding to the CDR3β loop of the CF34 TCR, and to a lesser degree the CDR3α loop, were observed in a number of CTL clones from unrelated individuals. The conserved selection of the length and sequence (16 amino acids, ASSFTWTSG GATDTQY) of the CDR3β loop, as well as sequence similarities in the CDR3α loop (AMREDTGNQFY), suggested that they might play a crucial role in determining the specificity of the CF34 TCR toward the HLA-B8-FLRGRAYGL complex. The CF34 TCR comprises *TRAV14*01* and *TRAJ49* combined with *TRBV11-2*03* and *TRBJ2*01*, quite distinct from the *TRAV26-2*01* and *TRBV7-8*03* gene segments used by the LC13 TCR (Argaet et al., 1994; Callan et al., 1998). Although their respective Vα chains only shared 28% sequence identity, their Vβ chains shared 59% sequence identity, and hence their CDR1β and CDR2β loops are similar. However, there was no sequence conservation between the CDR3 loop of the CF34 TCR and that of the LC13 TCR, thereby reflecting the very distinct nature of these TCRs.

The V_α and V_β domains of the CF34 TCR contributed 41.7% and 58.3%, respectively, to the BSA at the HLA-B8-FLRGRAYGL interface (Figures 2A and 2C), which immediately provided some insight into the Vβ bias of the CF34 TCR. Nevertheless, all six CDR loops of the CF34 TCR contributed to the interaction, albeit to differing degrees (Figure 2C). Namely, the germline-encoded CDR1β loop contributed marginally to the interaction (3.6% BSA), whereas the CDR1α, CDR2α, and CDR2β loops interacted to a greater extent (13%, 10.7%, and 11.9% BSA, respectively). The footprint was clearly dominated by the non-germline-encoded CDR3 loops (Table 2), and in particular the CDR3β loop, which contributed approximately 40% of the BSA at the interface, which was consistent with the repeated selection of this CDR3β sequence in unrelated individuals. It was notable that, although the Vα and Vβ domains of the LC13 TCR contributed roughly equally to the interaction with HLA-B8-FLRGRAYGL, mutagenesis studies showed that the non-germline-encoded CDR3 loops of the LC13 TCR dominated the energetic landscape of the interaction with HLA-B8-FLRGRAYGL (Borg et al., 2005).

As in the LC13 TCR-HLA-B8-FLRGRAYGL interaction (Kjer-Nielsen et al., 2003), the HLA-B8-FLRGRAYGL complex moved minimally (rmsd 0.28 Å for liganded and nonliganded HLA-B8-FLRGRAYGL) upon ligation with the CF34 TCR. The peptide did not change conformation appreciably, and movement in HLA-B8 was restricted to residues Glu58, Arg62, Glu72, Arg79, Glu154, Glu166, and Arg170 (data not shown) and either minimized steric hindrance or formed specificity-governing interactions with the CF34 TCR.

Given the very distinct footprints of the CF34 and LC13 TCRs, the detailed interactions that these TCRs make with their cognate HLA-B8-FLRGRAYGL target are markedly different from one another, and the centers of mass of the two TCRs are separated by 20 Å, (Figures 2A–2D). Accordingly, the CF34 Vα center of mass sits above Glu166 of HLA-B8 (Figures 2C and 3A), whereas the same point in LC13 sits over Val 152 (compare Figures 2C and 2D). The center of mass for CF34 Vβ is over Thr71 of HLA-B8, whereas for LC13 this resides over Gly16. The Vα domain of the CF34 TCR is positioned over the α2 helix, and CDR1α and CDR2α exclusively contact HLA-B8, whereas the CDR3α loop bridged the α1 and α2 helices and contacted the peptide (Figures 2C and 2D). CDR1α sits above the α2 helix of HLA-B8, in which Pro30α nestles between the long aliphatic side chains of Glu166, Trp167, and Arg170, which enables Ser28α^O to move close enough to hydrogen bond to Arg170$^{N\eta 2}$ as well as enabling Ser31α to make vdw contacts with Thr163 and Glu166 (Figure 3A, Table 2). The CDR2α loop also contacts the α2 helix of HLA-B8, such that the aromatic ring of Tyr59α lies flat against Gly162 and forms vdw contacts with Glu 166. Unusually, Gln61$\alpha^{O\epsilon 1}$ H bonded to Arg108$^{N\eta 2}$, a residue that is not located within the α helices of the Ag-binding cleft (Figure 3A). CDR3α, which contributes 18% BSA at the interface, docks above the α1 helix but also bridges across to the α2 helix, whereby Asp109$\alpha^{O\delta 2}$ H bonds to Trp167$^{N\epsilon 1}$ (Figure 3B). The CDR3α loop is flanked by the long side chains

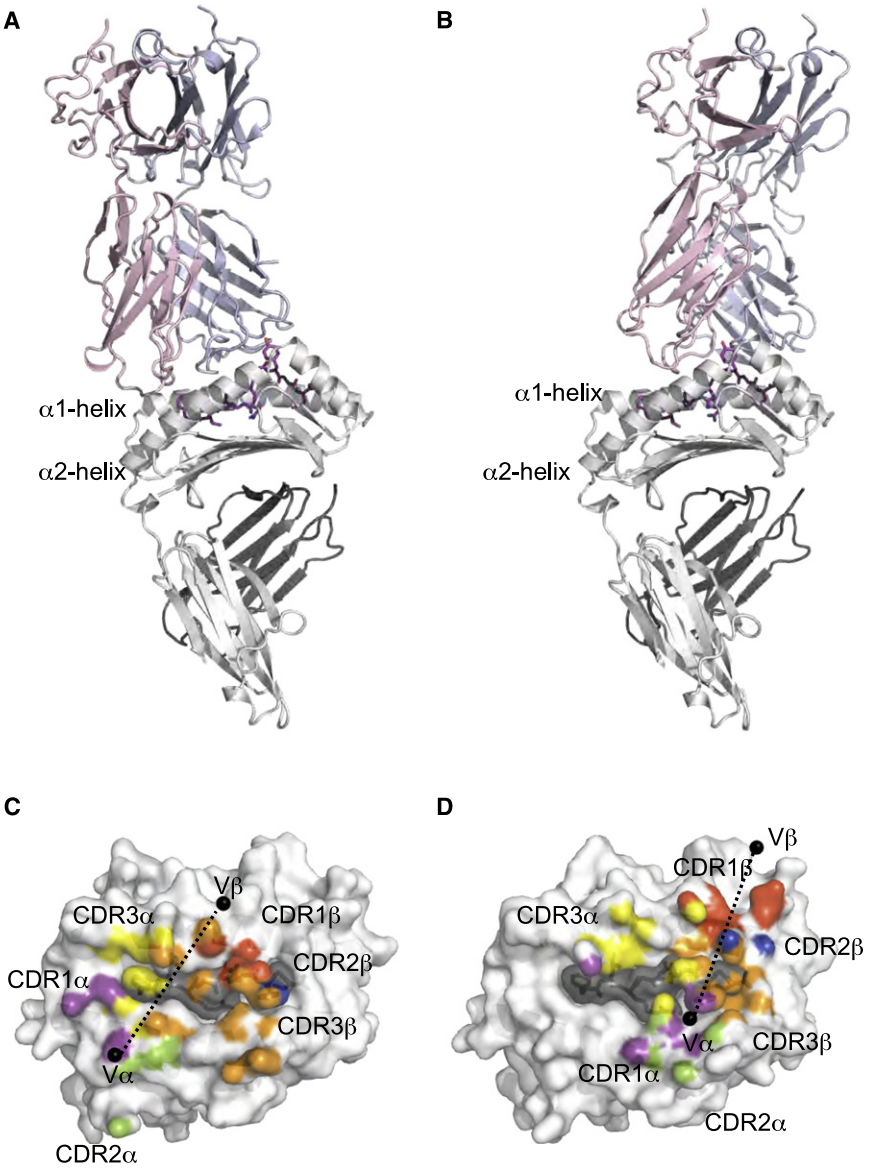

Figure 2. Footprint of CF34 and LC13 TCRs in Complex with HLA-B8-FLRGRAYGL

Ribbon representation of the CF34 TCR-HLA-B8-FLRGRAYGL complex (A) and the LC13 TCR-HLA-B8-FLRGRAYGL complex (B). The TCR α chain is in pale pink; the β-chain is in pale blue; HLA-B8 is in gray; and the FLRGRAYGL peptide is represented as a purple stick. The footprints of the CF34 TCR (B) and the LC13 TCR (B) on HLA-B8-FLRGRAYGL are shown. Residues contacted by the CDR loops are colored in purple (CDR1α), green (CDR2α), yellow (CDR3α), red (CDR1β), blue (CDR2β), and orange (CDR3β) in both complexes. The black spheres in (C) and (D) represent the orientation on the Vα and Vβ chains of each TCR on the HLA-B8-FLRGRAYGL complex, as calculated from the center of mass.

of Arg62 and Glu58, forming vdw contacts with Thr110α, Gly111α and Asn112α as well as Gly111α^{O} H-bonding to Arg62$^{N\epsilon,\ N\eta2}$ (Figure 3B). The CDR3α loop is flanked by the long side chains of Arg62 and Glu58 from the HLA-B8 molecule. These residues make vdw contacts with Thr110α, Gly111α, and Asn112α of the CDR3α loop, and there are also hydrogen bonds between Arg62$^{N\epsilon,\ N\eta2}$ and Gly111α^{O} (Figure 3B).

The Vβ domain of the CF34 TCR is positioned over the α1 helix. Although the CF34 TCR CDR1β loop sequence (SGHAT) is similar to that of the LC13 TCR (SGHVS), the former exclusively contacted the peptide, whereas the latter interacted marginally with HLA-B8. The CDR2β loop (FQNNGV) of the CF34 TCR contacts both the peptide and the α1 helix of HLA-B8, whereas the LC13 TCR CDR2β loop (FQNEAQ) solely contacts the α1 helix of HLA-B8. The CF34 TCR residue Gln 57β, from the CDR2β loop, makes H bonds and forms vdw interactions with Thr73 and Thr69, respectively, and these bonds are supplemented by the neighboring framework residues, Val66β and Asp67β, which interact with Gln65 and Thr69 (Figure 3C). The CDR3β loop dominated the contacts with the α1 and α2 helices (Figure 3D), as well as the peptide (discussed below). The 16-amino-acid-long CDR3β loop, which included a non-germline-encoded ^{108}Phe-Thr-Trp^{110} motif, engenders a very broad footprint that spans most of the length of the HLA-B8 Ag-binding cleft. There is one H bond between Ser112β^{O} and Tyr159^{N} HLA-B8, whereas vdw forces dominate the remainder of the interactions. Phe108α and Trp110α make a marked contribution to the vdw contacts; the former packs against the aliphatic chain of Arg151 and Ala150, whereas the latter is wedged above the α1 helix and interacts with Arg62, Ile66, and Thr69. In addition, the tip (^{112}Ser-Gly-Gly^{114}) of the CDR3β loop as well as Thr116β make a number of vdw contacts (Figure 3D).

Accordingly, the CF34 TCR binds extensively to HLA-B8 in a manner that is distinct from that of the LC13 TCR; this binding mode includes differing relative contributions and positioning of the CDR loops.

Interactions with the Peptide

The FLRGRAYGL epitope protruded minimally from HLA-B8 (Kjer-Nielsen et al., 2002a) and as such contributed only 20% of the buried surface area of the pMHC interface in both the LC13 TCR and the CF34 TCR ligated complexes. The side chains of the peptide that are exposed for TCR contact are P1^{Phe}, P6^{Ala}, and P7^{Tyr}, as well as the main chain of P4^{Gly} and P8^{Gly} (Figures 3E and 3F). LC13 TCR focused exclusively on positions P6–P8, and P7^{Tyr} was fully occluded by CDR1α and both CDR3 loops (Kjer-Nielsen et al., 2003 and Figure 3E). The small side chains at positions P6 and P8 were critical for enabling P7^{Tyr} to sit deep within the LC13 TCR binding pocket as well as for making specificity-governing interactions (Figure 3E). This mode of binding was

Table 2. Contacts between CF34 and HLA-B8-FLRGRAYGL

	TCR Residue	MHC Residue	Bond Type	Gene Segment
CDR1α	Ser^{38}	Arg^{170}	vdw	Vα
	$Ser^{28\text{-}O}$	$Arg^{170\text{-}N\eta2}$	HB	Vα
	Asp^{29}	Arg^{170}	vdw	Vα
	Pro^{30}	Trp^{167}, Arg^{170}	vdw	Vα
	Ser^{31}	Thr^{163}, Glu^{166}	vdw	Vα
CDR2α	Tyr^{59}	Ala^{158}, Gly^{162}, Glu^{166}	vdw	Vα
	Gln^{61}	Arg^{108}	vdw	Vα
	$Gln^{61\text{-}O\epsilon1}$	$Arg^{108\text{-}N\eta2}$	HB	Vα
CDR3α	Asp^{109}	Arg^{62}, Thr^{163}, Trp^{167}	vdw	N-Jα
	$Asp^{109\text{-}O\delta2}$	$Trp^{167\text{-}N\epsilon1}$	HB	N-Jα
	Thr^{110}	Glu^{58}, Tyr^{59}, Arg^{62}	vdw	Jα
	Gly^{111}	Arg^{62}	vdw	Jα
	$Gly^{111\text{-}O}$	$Arg^{62\text{-}N\eta2\text{-}N\epsilon}$	HB	Jα
	Asn^{112}	Arg^{62}	vdw	Jα
CDR2β	$Gln^{57\text{-}O\epsilon1}$	$Thr^{73\text{-}O\gamma1}$	HB	Vβ
	Gln^{57}	Thr^{69}	vdw	Vβ
FW	Val^{66}	Gln^{65}, Thr^{69}	vdw	Vβ
	$Val^{66\text{-}O}$	$Gln^{65\text{-}N\epsilon2}$	H	Vβ
	Asp^{67}	Gln^{65}	vdw	Vβ
	$Asp^{67\text{-}O\delta2}$	$Gln^{65\text{-}N\epsilon2}$	HB	Vβ
CDR3β	Phe^{108}	Ala^{150}, Arg^{151}	vdw	Vβ–N
	Thr^{109}	Gln^{155}	vdw	N
	Trp^{110}	Arg^{62}, Ile^{66}, Thr^{69}	vdw	N-Dβ
	Ser^{112}	Gln^{155}, Ala^{158}, Tyr^{159}, Thr^{163}	vdw	Dβ
	$Ser^{112\text{-}O}$	$Tyr^{159\text{-}N}$	HB	Dβ
	Gly^{113}	Thr^{163}	vdw	Dβ
	Gly^{114}	Ala^{158}	vdw	Dβ
	Thr^{116}	Glu^{154}, Gln^{155}	vdw	Jβ
	TCR Residue	Peptide Residue	Bond Type	Gene Segment
CDR3α	Asp^{109}	Phe^{1}	vdw	N-Jα
CDR1β	Gly^{28}	Tyr^{7}	vdw	Vβ
	$Gly^{28\text{-}O}$	$Tyr^{7\text{-}OH}$	HB	Vβ
	His^{29}	Tyr^{7}	vdw	Vβ
	Ala^{30}	Ala^{6}, Tyr^{7}	vdw	Vβ
	$Ala^{30\text{-}N}$	$Tyr^{7\text{-}OH}$	HB	Vβ
CDR2β	Gln^{57}	Arg^{5}, Ala^{6}	vdw	Vβ
	Asn^{58}	Ala^{6}	vdw	Vβ
	$Asn^{58\text{-}O\delta1}$	$Ala^{6\text{-}O}$	HB	Vβ
CDR3β	Phe^{108}	Ala^{6}, Tyr^{7}	vdw	Vβ–N
	Thr^{109}	Ala^{6}	vdw	N
	Thr^{111}	Gly^{4}	vdw	Dβ

Subscripted designations indicate the atom involved in hydrogen bonding. Abbreviations are as follows: FW, Framework residue; HB, hydrogen bond; V, variable; N, non-germline encoded; D, diversity; J, joining; vdw, van der Waals cutoff distance $\leq$ 4 Å.

fully consistent with the peptide substitution data, which revealed that positions P6–P8 were critical for the interaction, whereas the $P1^{Phe}$ position was not (Kjer-Nielsen et al., 2003).

In contrast, the CF34 TCR interacted with positions $P1^{Phe}$, $P4^{Gly}$, $P5^{Arg}$, $P6^{Ala}$, and $P7^{Tyr}$ of the peptide, and contacts were mediated by the CDR3α, CDR1β, CDR2β, and CDR3β loops (Figure 3F). $P7^{Tyr}$ is only partially buried (70%) by the CF34 TCR and makes contacts with the CDR1β and CDR3β. Here, Phe108β formed vdw contact with $P7^{Tyr}$, whereas CDR1β contacted $P7^{Tyr}$ via Gly28β, Ala30β, and the main chain of His29β principally by vdw interactions, but a hydrogen bond is also formed between the $P7^{Tyr\text{-}OH}$ and the main chain of $Gly28\beta^{O}$ and $Ala30\beta^{N}$ (Figure 3F). $P6^{Ala}$ of the FLRGRAYGL peptide is buried between the three CDR loops of the CF34 TCR Vβ chain. $P6^{Ala}$ forms a large number of vdw interactions and one hydrogen bond between $P6^{Ala\text{-}O}$ and $Asn58\beta^{O\delta1}$ of CDR2β (Table 2). $P5^{Arg}$ and $P4^{Gly}$ are in contact with the CF34 TCR via their main chain and interact with CDR2β and CDR3β, respectively. $P1^{Phe}$ is contacted by non-germline-encoded Asp109α, which sits atop $P1^{Phe}$ to fully bury it. This interaction is stabilized by a hydrogen bond between $Asp109\alpha^{O\delta2}$ and $Trp167^{N\epsilon1}$ as well as H bonding between the main chain of $Asp109\alpha^{O}$ H and $Arg62^{N\epsilon}$ of HLA-B8 (Figure 3F). The observed interactions correlate with the ability of the CF34 TCR to accommodate substitutions at the $P8^{Gly}$ while being sensitive to substitutions at $P7^{Tyr}$ and $P1^{Phe}$ (Figure 1).

Thus, whereas the LC13 TCR focuses on the C-terminal end, the CF34 TCR is focused on the N-terminal region of the FLRGRAYGL epitope.

Differing Docking Footprints

The crystal structures of the CF34 and LC13 TCRs in complex with HLA-B8-FLRGRAYGL allowed us to compare their features in relation to those of other TCRs that also recognize the same pMHC. Other examples of previously studied TCRs that can recognize the same pMHC include the A6 TCR (Garboczi et al., 1996) and B7 TCR (Ding et al., 1998), which recognize $HLA\ A2^{TAX}$; B3K506 TCR, YAe62 TCR, and 2W2D TCR, which recognize $I\text{-}Ab^{3K}$ (Dai et al., 2008); and 172.10 TCR (Maynard et al., 2005), 1934.4 TCR, and CL19 TCR (Feng et al., 2007), which recognize $I\text{-}Au^{MBP1\text{-}11}$. Although the detailed interactions within each of these respective complexes varied, the positioning of the TCR remained relatively fixed *within* the particular pMHC system (Figures 4A–4C). However, the CF34 TCR was obviously more N-terminally focused with respect to the LC13 TCR in its recognition of HLA-B8-FLRGRAYGL (Figure 4D).

Of the 19 unique TCR-pMHC-I structures solved to date, only four TCRs contact the P1 position of the peptide; these four TCRs are the A6 (Garboczi et al., 1996) and B7 (Ding et al., 1998) TCR -HLA $A2^{TAX}$ complexes, the scKB5-C20 TCR-$H2\text{-}K^{b\text{-}pKB1}$ complex (Reiser et al., 2002), and the ELS4 TCR-$HLA\text{-}B*3501^{EPLP}$ complex (Tynan et al., 2007). Thus, the N-terminal peptide focus of CF34 TCR is somewhat atypical of TCR-pMHC-I structures. Indeed, the CF34 TCR footprint on HLA-B8-FLRGRAYGL was more N-terminally focused than any TCR-pMHC-I complex determined to date and was more reminiscent of the N-terminal focus of the class-II-restricted autoimmune TCR complexes (Deng and Mariuzza, 2007) (Figure 4E). Indeed, there are similarities in the docking mode of the CF34 TCR and the 3A6 autoreactive TCR that docked onto HLA DR2 bound to the $MBP_{87\text{-}99}$ peptide (Li et al., 2005), as shown by the positioning of the different CDR loops over the pMHC landscape (compare Figure 4E).

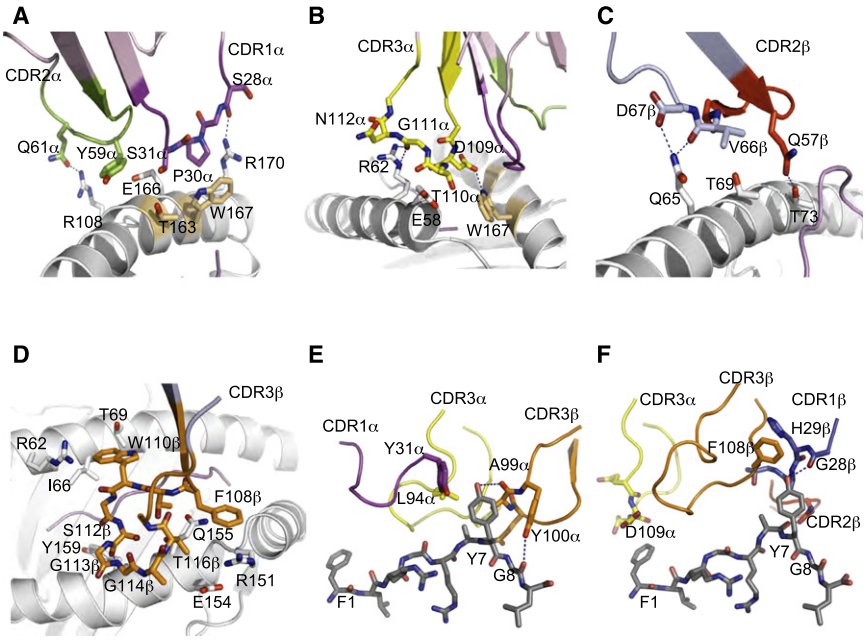

Figure 3. CF34 Contacts with HLA-B8-FLRGRAYGL and Comparison to LC13

Contacts between the HLA-B8-FLRGRAYGL complex and CDR2α (A), CDR3α (B), CDR2β (C), and CDR3β (D) are shown, and the HLA-B8 and selected side chains are depicted in gray. CDR loops and selected side chains are colored as in Figure 2. Comparison of LC13 and CF34 interactions with the FLRGRAYGL peptide (E and F) are shown. The CDR loops of LC13 (E) and CF34 (B) are shown interacting with the exposed side chains of the FLRGRAYGL peptide in gray. The indicated CDR loops are colored, and H bonds to the hydroxyl group of the P7 Tyr are shown as dotted lines. Residues Phe1 (F1), Tyr7 (Y7), and Gly8 (G8) of the FLRGRAYGL peptide are labeled.

Accordingly, the cognate CF34 TCR-HLA-B8 interaction is a little unusual when compared to other antiviral TCR-pMHC structures and is more similar to autoreactive TCR-pMHC complexes that exhibited an N-terminal footprint.

A Consensus N-terminal Footprint

Because the CF34 TCR displayed an N-terminal footprint with sensitivity to substitutions to $P1^{Phe}$, we established whether this $P1^{Phe}$ specificity was a general trend for CTL clones in HLA-$B8^{+}B44^{+}$ individuals, as indicated previously (Burrows et al., 1995). To evaluate this, we compared the specificities of an archetypal LC13-like CTL clone from an HLA-$B8^{+}$, $B44^{-}$ individual and seven CTL clones from HLA-$B8^{+}$, $B44^{+}$ individuals by using cytotoxicity assays and a large panel of analogs of the FLRGRAYGL peptide with substitutions at P1 and P8. The CTL clone SC17 from the HLA-$B8^{+}$ individual expressed a TCR amino acid sequence identical to that of the LC13 TCR (Argaet et al., 1994); its TCR showed specificity toward the $P8^{Gly}$ position and was insensitive to substitutions at the $P1^{Phe}$ position. Conversely, the CF34 TCR was shown to be insensitive to substitutions at P8 and yet was markedly specific toward $P1^{Phe}$ (Figure 5A). The CTL clones CF27 and PP36 from HLA-$B8^{+}B44^{+}$ individuals exhibited a similar specificity profile to that of the CF34 CTL clone in the CTL killing assays, suggesting a similar docking footprint among these CTL clones. However, not all CTL clones from HLA-$B8^{+}B44^{+}$ individuals exhibited this "CF34 TCR specificity profile." For example, the JL14 and CF8 CTL clones exhibited a specificity profile that was more "LC13 TCR-like," whereas the RL42 CTL clone exhibited sensitivity to substitutions at both the P1 and P8 positions (Figure 5A). Collectively, these data indicated that although there was a propensity for CTL clones from HLA-$B8^{+}B44^{+}$ individuals to focus on the N terminus of the FLRGRAYGL determinant, other CTLs from these individuals adopted alternative strategies to avoid self-HLA-B44 reactivity.

To gain an understanding of the relationship between the N-terminal footprint adopted by the CF34 TCR on HLA-B8-FLRGRAYGL and the acquisition of tolerance to the trans HLA-B44 allotype, we compared the Ag-binding surfaces of HLA-B8 and HLA-B44. There are 24 polymorphisms between HLA-B44 and HLA-B8, and only five of these map to the α helices of the Ag-binding surface (HLA-B8→HLA-B44; Asn→Thr80, Arg→Leu82, Gly→Arg83, Thr→Leu163 and Trp→Ser167) (Macdonald et al., 2003; Reid et al., 1996a). These sites are clustered at the N terminus and the C terminus of the Ag-binding cleft, as highlighted in cyan in Figure 5B, depicting the CDR loops of CF34 overlying HLA-B8. Notably, the polymorphism that distinguishes HLA-B8 and HLA-B44 at the N-terminal region (Thr→Leu163 and Trp→Ser167) maps to a sizeable contact point (12.3% of HLA-B8 buried surface area) with the CF34 TCR, specifically via the CDR1α, CDR3α, and CDR3β loops (Figure 5B). In the LC13 complex with HLA-B8-FLRGRAYGL, neither Trp167 nor Thr163 makes contacts with the TCR, whereas for CF34 Thr163 is contacted by CDR1α (Ser31α), CDR3α (Asp109α), and CDR3β (Ser112β and Gly113β). Moreover, Trp167 interacts with CDR1α (Pro30α) and CDR3α (Asp109α) (Figure 5B). Thus, the CF34 TCR focuses on the N-terminal region of HLA-B8 and makes extensive contacts in an area that diverges from the HLA-B44 allotype, creating potentially unfavorable interactions that are predicted to prevent cross-reaction with the HLA-B44 molecule.

DISCUSSION

We have provided a basis for how the T cell repertoire maintains self-pMHC tolerance without compromising immune function in a naturally out-bred population. Specifically, our findings demonstrate the structural basis of the avoidance of self-MHC reactivity in the CTL response to HLA-B8-FLRGRAYGL in heterozygous HLA-$B8^{+}$, $B44^{+}$ individuals (Burrows et al., 1995). Unlike the prototypic LC13 TCR, the CF34 TCR displayed heightened specificity for the $P1^{Phe}$ position, and we have provided a structural basis for this specificity shift. In previous examples of different TCRs that recognize the same pMHC (HLA $A2^{TAX}$, I-Au^{MBP}, and I-Ab^{3K}) (Dai et al., 2008; Ding et al., 1998; Feng et al., 2007; Garboczi et al., 1996; Maynard et al., 2005), the comparative modes of TCR docking were broadly

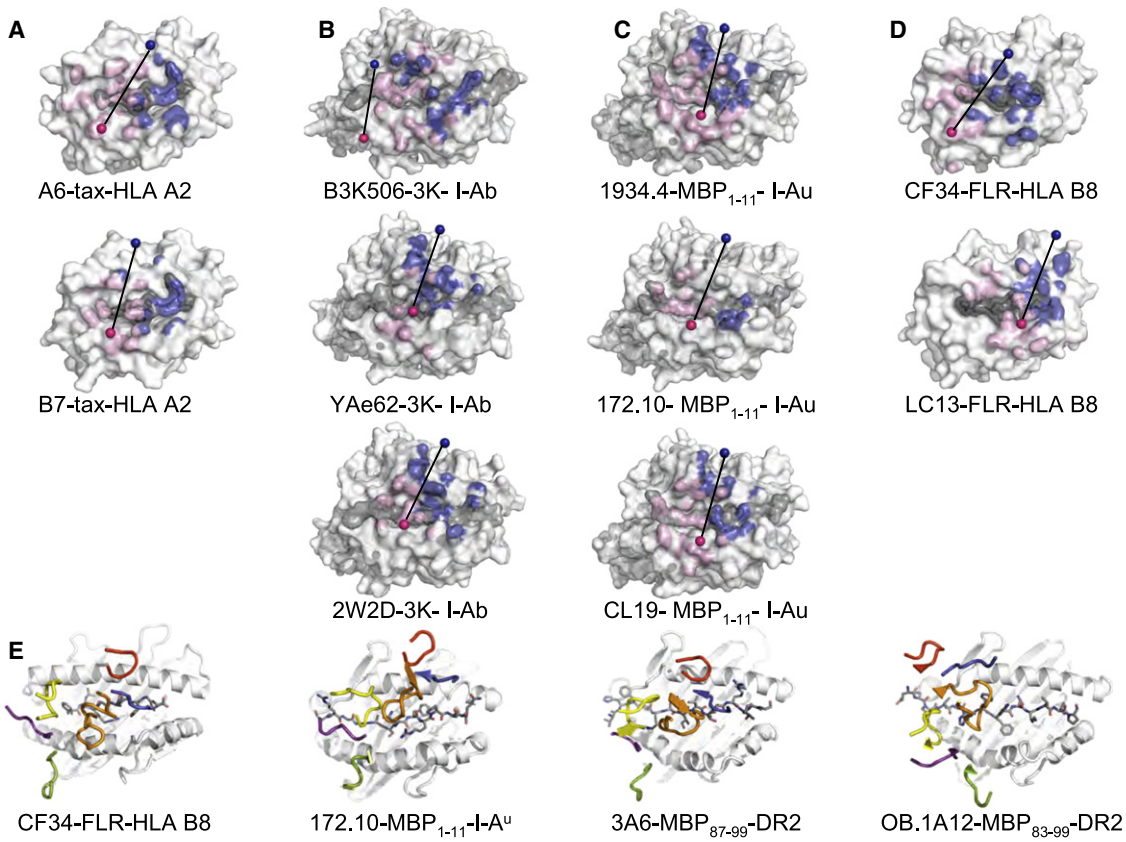

Figure 4. Footprints of TCRs that Recognize the Same pMHC Complex

Space-filling models of pMHC complexes recognized by more than one TCR are shown. (A) Footprint of the A6 and B7 TCRs on the surface of HLA $A2^{TAX}$. (B) The footprint of B3K506, YAe62, and 2W2D TCRs on the surface of the $I\text{-}Ab^{3K}$. (C) The footprint of 1934.4, 172.10, and CL19 TCRs on the $I\text{-}Au^{MBP1\text{-}11}$. (D) The footprint of CF34 and LC13 TCR on the HLA-B8-FLRGRAYGL. The CDR loops of the α chain are represented in pink, and the β chain is in blue. The spheres represent the center of mass for the Vα chain in pink and for the Vβ chain in blue. (E) Docking similarity of CF34 with autoimmune TCRs bound to pMHC-II. CDR loops (in color) of the indicated TCRs are shown overlying their cognate pMHC complexes (gray with stick peptides). CF34 and three autoimmune TCRs, 172.10, 3A6, and OB.1A12, that recognize an MBP peptide bound to a MHC class II molecule are shown. Note that the N-terminal docking focus of the MHC class II-restricted TCRs resembles the focus of CF34. Similarity in the orientation and conformation of the CDR loops of 3A6 and CF34 is evident.

similar within each pMHC group. In contrast, the footprint of the CF34 TCR is markedly N-terminally shifted with respect to the LC13 TCR footprint on HLA-B8-FLRGRAYGL. Given that the CF34 TCR is selected because of the need to avoid self-HLA-B44 reactivity, the N-terminal footprint of this cognate antiviral CF34 TCR-HLA-B8-FLRGRAYGL reveals that unusual N-terminal docking footprints are not restricted to autoreactive TCRs (Deng and Mariuzza, 2007; Hahn et al., 2005; Li et al., 2005; Nicholson et al., 2005). Conversely, it will be interesting to evaluate whether autoreactive TCRs can also adopt more "canonical" footprints.

The CF34 footprint on HLA-B8-FLRGRAYGL appears representative of a sizeable proportion of the T cell repertoire in $HLA\text{-}B8^{+}B44^{+}$ individuals, indicating a significant reshaping of the TCR repertoire selected in the face of the trans HLA-B44 self-complex. This repertoire refocusing exhibits biased Vβ usage in unrelated individuals, as reflected in the CF34 TCR, and conservation of the CDR3β loop was consistent with its prominent role in interacting with the FLR peptide. Importantly, approximately 50% of the CTL clones tested, which display differing Vα and/or Vβ usage in comparison to CF34 TCR, exhibit the same specificity profile as the CF34 TCR; specifically, they are insensitive to substitutions at $P8^{Gly}$ and sensitive to substitutions at $P1^{Phe}$. However, as judged by the peptide substitution analysis, not all CTL clones in $HLA\text{-}B8^{+}B44^{+}$ individuals are predicted to use a footprint similar to that of CF34 TCR, thereby highlighting the versatility of the T cell repertoire in $HLA\text{-}B8^{+}B44^{+}$ individuals. The CF34 N-terminal footprint coincided with the area of polymorphism between HLA-B44 and HLA-B8, and this probably reflects the need for CF34 to monitor these differences to avoid self-reactivity toward HLA-B44. It will be of interest to establish how other CTL clones that exhibit $P8^{Gly}$ specificity will dock onto HLA-B8-FLRGRAYGL. In this regard, it was notable that the other site of HLA-B8/B44 polymorphism maps to the C terminus of the Ag-binding cleft that is proximal to $P8^{Gly}$. Although the LC13 TCR forms one vdw interaction (via Val30β) with a site (Asn80) that maps to this C-terminal polymorphic region, alanine-scanning mutagenesis has indicated that this region is not energetically important for the LC13 TCR-HLA-B8-FLRGRAYGL interaction (Borg et al.,

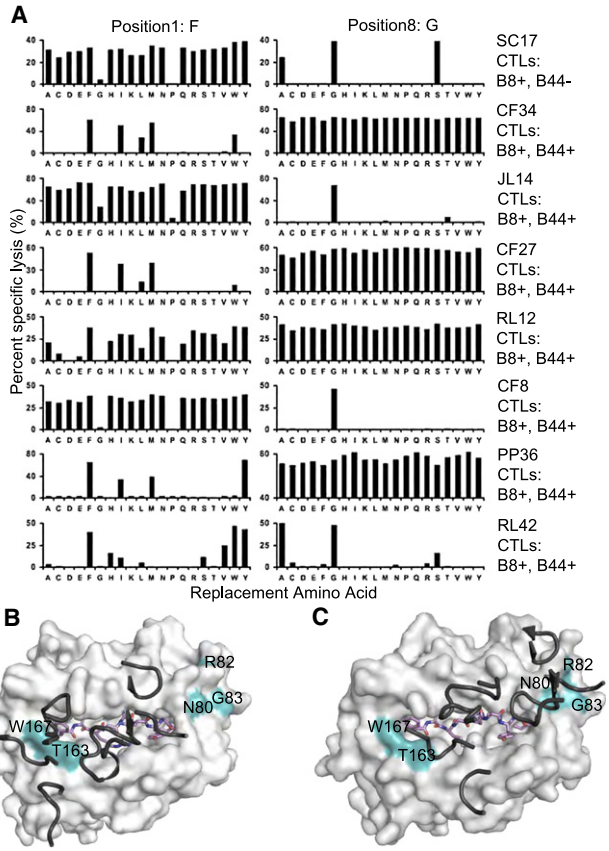

Figure 5. Consensus Footprints in HLA-B8$^+$B44$^+$ Individuals

(A) FLR-reactive T cells from HLA-B8$^+$, B44$^+$ individuals can frequently tolerate peptide amino acid substitutions at P8 but not at P1, suggesting TCR docking over the peptide N terminus. Recognition by nine different FLR-reactive CTL clones (listed on the right) of monosubstituted analogs of the EBV peptide FLRGRAYGL, in which every one of the 20 genetically coded amino acids were substitutes at P1 or P8. The horizontal axis lists the residue replacing the parent residue. Target cells were HLA-B8$^+$ PHA blasts, the peptide concentration was 0.1 μM, and the E:T was 1:1. The SC17 CTL clone was from an HLA-B8$^+$, B44$^-$ individual, and it expresses the well-characterized LC13 TCR. All other CTL clones are from individuals who coexpress HLA-B8 and HLA-B44. Analogous data were observed when these experiments were repeated for a second time. The docking footprints of the CF34 TCR (B) and LC13 TCR (C) are shown with CDR loops in gray overlying HLA-B8-FLRGRAYGL. Surface polymorphisms that distinguish HLA-B8 and HLA-B44 are lettered and shown in cyan.

2005). Our observations regarding the CF34 TCR resonate with the observations in the alloreactive 2C TCR system, where the 2C TCR was observed to adopt two differing footprints in recognizing the "cognate" complex in comparison to the alloreactive H2-L^d complex (Colf et al., 2007).

Here, we provide fundamental insights into how the need for self-tolerance reshapes the TCR repertoire toward a defined viral determinant thus avoiding self-HLA reactivity. Specifically, to avoid autoreactivity on HLA-B44, the CF34 focuses on the HLA-B8 N-terminal region that differs from that of HLA-B44. Thus, "seeing the differences" simultaneously provides a mechanism for the avoidance of autoreactivity and highlights the versatility of the T cell repertoire and TCR-pMHC interaction.

EXPERIMENTAL PROCEDURES

Cell Lines

CTL clones were generated from healthy EBV-exposed individuals by agar cloning as previously described (Burrows et al., 1995). The FLR-reactive CTL clone SC17 has been previously described (Argaet et al., 1994) and is from an HLA-B8$^+$, B44$^-$ individual (HLA-A1, A31, B8, B51). It expresses the well-characterized LC13 TCR (Argaet et al., 1994) (Kjer-Nielsen et al., 2003). Other FLR-reactive CTL clones are from individuals who coexpress HLA-B8 and HLA-B44, including CF40, CF8, RL42 (Burrows et al., 1995), and PP7 (Burrows et al., 1997b), which have been previously described. Clone CF40 expresses the CF34 TCR (Burrows et al., 1995). Clones JL14, CF27, RL12, and PP36 have not been previously described but are known to be FLR reactive but not cross-reactive with HLA-B44 (data not shown). PHA blasts were generated and maintained as previously described (Burrows et al., 1995).

Cytotoxicity Assay

CTL clones were tested in duplicate for cytotoxicity in the standard 5 hr chromium release assay (E/T ratio of 1:1) as previously described (McCluskey et al., 1986). In brief, CTLs were assayed against ^{51}Cr-labeled PHA blast targets that were pretreated with the peptide (0.1 μM for 1 hr). A beta scintillation counter (Topcount Microplate; Packard Instrument Co., Meriden, CT) was used for measuring ^{51}Cr levels in assay supernatant samples. The mean spontaneous lysis for target cells in culture medium was <20%, and the variation about the mean specific lysis was <20%.

Protein Expression, Purification, and Crystallization

The CF34 TCR was expressed, refolded, and purified with an engineered disulfide linkage in the constant domains between the TRAC and TRBC. Both the α and β chains of the CF34 TCR were expressed separately as inclusion bodies in a BL21 *Escherichia coli* strain. Inclusion bodies were resuspended in 8 M urea, 20 mM Tris-HCl (pH 8), 0.5 mM Na-EDTA, and 1 mM DTT. CF34 TCR was refolded by flash dilution in a solution containing 5 M urea, 100 mM Tris (pH 8), 2 mM Na-EDTA, 400 mM L-arginine-HCl, 0.5 mM oxidized glutathione, 5 mM reduced glutathione, and complete EDTA-free (anti-protease cocktail) so that any degradation of the α chain would be avoided. The refolding solution was then dialyzed so that urea would be eliminated. The resulting protein solution was then purified by gel filtration and HiTrap-Q anion exchange chromatography. The LC13 TCR was produced under conditions similar to those used for the CF34 TCR.

Soluble class I heterodimers containing the FLR peptide (or the peptide mutated) were prepared as described previously (Clements et al., 2002; Reid et al., 1996b). In brief, the truncated forms (amino acid residues 1–276) of the HLA-B8 heavy chain and full-length β2-microglobulin (β2 m) were expressed in *Escherichia coli* as inclusion bodies. The complex of HLA-B8-peptide was refolded by dilution of the heavy chain and β2 m inclusion body preparations into refolding buffer containing a molar excess of peptide ligand. The refolded complexes were concentrated and purified by anion exchange chromatography. The complexes were further purified by gel filtration and HiTrap-Q anion exchange chromatography.

Purified HLA-B8-FLRGRAYGL was mixed with an excess of purified CF34 TCR, and then the CF34-HLA-B8-FLRGRAYGL complex was purified with a Sephadex-200 gel filtration column.

Crystallization

Crystals of the CF34-HLA-B8-FLRGRAYGL complex were grown by the hanging-drop, vapor-diffusion method at 20°C with a protein/reservoir drop ratio of 1:1 at a concentration of 11 mg/ml in 10 mM Tris (pH 8) and 150 mM NaCl. Large rod-shaped crystals grew with 11% PEG 20K, 0.2 M Li_2SO_4, 0.1 M Tris (pH 8.4), 6 mM CdCl, 4% ethylene glycol, and 4% dioxane.

Data Collection and Structure Determination

The CF34-HLA-B8-FLRGRAYGL crystals were soaked in a cryoprotectant solution containing mother liquor solution with the PEG concentration increased to 25% (w/v) and then flash frozen in liquid nitrogen. Data were collected on the 3BM1 beamline at the Australian Synchrotron, Clayton with the ADSC-Quantum 210 CCD detector (at 100K). Data were processed with

the MOSFLM software (Leslie, 1992) and scaled with SCALA software (Evans, 2006) from the CCP4 suite (CCP4, 1994).

The CF34-HLA-B8-FLRGRAYGL crystal belonged to the space group *I222* with unit cell dimensions (Table 1), consistent with two complexes in the asymmetric unit. The structure was determined by molecular replacement with the PHASER (Read, 2001) program, for which the LC13 TCR served as the search model for the TCR (Protein Data Bank accession number, 1KGC) (Kjer-Nielsen et al., 2002b) and the HLA-B8-FLRGRAYGL served as the MHC model without the peptide (Protein Data Bank accession number, 1M05) (Kjer-Nielsen et al., 2002a). Manual model building was conducted with the O software (Jones et al., 1991) followed by maximum-likelihood refinement with the REFMAC 5 program (CCP4, 1994). "Translation, liberation and screw rotation" displacement refinement was used for modeling anisotropic displacements of defined domains, and medium noncrystallographic symmetry (NCS) restraints were also used during the refinement process. The TCR was numbered according to the IMGT unique numbering system (Lefranc et al., 2005), whereby the CDR1 loops start at residue number 27, the CDR2 loops start at number 56, and the CDR3 loops start at residue number 105. The final model was validated with the Protein Data Base validation website, and the final refinement statistics are summarized in Table 1.

All molecular graphics representations were created using PyMol (DeLano, 2002).

Surface Plasmon Resonance Measurement and Analysis

All surface plasmon resonance experiments were conducted at 25°C on the BIAcore 3000 instrument with HBS buffer (10 mM HEPES [pH 7.4], 150 mM NaCl, and 0.005% surfactant P20). The HBS buffer was supplemented with 1% BSA so that nonspecific binding would be prevented. The human TCR-specific monoclonal antibody, 12H8 (Borg et al., 2005), was coupled to research-grade CM5 chips with standard amine coupling. For each experiment, CF34 was passed over the flow cell 4 and LC13 was passed over the flow cell 2 until approximately 200–400 response units were captured by the antibody. The other two flow cells were used as control cells for each experiment. The HLA-B8, either in complex with the wild-type or a variant peptide, was injected over all four flow cells at a rate of 20 μl/min, and there was a concentration range of 0.78–200 μM. The final response was calculated by subtraction of the response of the antibody alone from that of the antibody CF34 or LC13 complex. The antibody surface was regenerated between each analyte injection with Actisep (Sterogene). All experiments were conducted at least in duplicate.

BIAevaluation Version 3.1 was used for data analysis; the 1:1 Langmuir binding model was modified to include an additional parameter for the drifting baseline for the TCR capture by 12H8 was used for calculating the kinetic constants.

ACCESSION NUMBERS

The coordinates of the CF34-HLA-B8-FLRGRAYGLcomplex have been deposited in the Protein Data Bank under accession number 3FFC.

SUPPLEMENTAL DATA

Supplemental Data include one table and are available with this article online at http://www.immunity.com/supplemental/S1074-7613(09)00061-2.

ACKNOWLEDGMENTS

We thank the staff at the Australian synchrotron for assistance with data collection. The National Health and Medical Research Council (NHMRC) of Australia, Roche Organ Transplantation Research Foundation, and the Australian Research Council (ARC) supported this research. S.R.B. and A.W.P. are supported by NHMRC Senior Research Fellowships, and J.R. is supported by an ARC Federation Fellowship.

Received: September 29, 2008
Revised: November 14, 2008
Accepted: November 26, 2008
Published online: January 22, 2009

REFERENCES

CCP4 (Collaborative Computational Project, Number 4). (1994). The CCP4 suite: Programs for protein crystallography. Acta Crystallogr. D Biol. Crystallogr. *50*, 760–763.

Archbold, J.K., Macdonald, W.A., Burrows, S.R., Rossjohn, J., and McCluskey, J. (2008). T-cell allorecognition: a case of mistaken identity or déjá-vu? Trends Immunol. *29*, 220–226.

Argaet, V.P., Schmidt, C.W., Burrows, S.R., Silins, S.L., Kurilla, M.G., Doolan, D.L., Suhrbier, A., Moss, D.J., Kieff, E., Sculley, T.B., and Misko, I.S. (1994). Dominant selection of an invariant T cell antigen receptor in response to persistent infection by Epstein-Barr virus. J. Exp. Med. *180*, 2335–2340.

Arstila, T.P., Casrouge, A., Baron, V., Even, J., Kanellopoulos, J., and Kourilsky, P. (1999). A direct estimate of the human alphabeta T cell receptor diversity. Science *286*, 958–961.

Borg, N.A., Ely, L.K., Beddoe, T., Macdonald, W.A., Reid, H.H., Clements, C.S., Purcell, A.W., Kjer-Nielsen, L., Miles, J.J., Burrows, S.R., et al. (2005). The CDR3 regions of an immunodominant T cell receptor dictate the 'energetic landscape' of peptide-MHC recognition. Nat. Immunol. *6*, 171–180.

Burrows, S.R., Khanna, R., Burrows, J.M., and Moss, D.J. (1994). An alloresponse in humans is dominated by cytotoxic T lymphocytes (CTL) cross-reactive with a single Epstein-Barr virus CTL epitope: Implications for graft-versus-host disease. J. Exp. Med. *179*, 1155–1161.

Burrows, S.R., Sculley, T.B., Misko, I.S., Schmidt, C., and Moss, D.J. (1990). An Epstein-Barr virus-specific cytotoxic T cell epitope in EBV nuclear antigen 3 (EBNA 3). J. Exp. Med. *171*, 345–349.

Burrows, S.R., Silins, S.L., Cross, S.M., Peh, C.A., Rischmueller, M., Burrows, J.M., Elliott, S.L., and McCluskey, J. (1997a). Human leukocyte antigen phenotype imposes complex constraints on the antigen-specific cytotoxic T lymphocyte repertoire. Eur. J. Immunol. *27*, 178–182.

Burrows, S.R., Silins, S.L., Khanna, R., Burrows, J.M., Rischmueller, M., McCluskey, J., and Moss, D.J. (1997b). Cross-reactive memory T cells for Epstein-Barr virus augment the alloresponse to common human leukocyte antigens: Degenerate recognition of major histocompatibility complex-bound peptide by T cells and its role in alloreactivity. Eur. J. Immunol. *27*, 1726–1736.

Burrows, S.R., Silins, S.L., Moss, D.J., Khanna, R., Misko, I.S., and Argaet, V.P. (1995). T cell receptor repertoire for a viral epitope in humans is diversified by tolerance to a background major histocompatibility complex antigen. J. Exp. Med. *182*, 1703–1715.

Callan, M.F., Annels, N., Steven, N., Tan, L., Wilson, J., McMichael, A.J., and Rickinson, A.B. (1998). T cell selection during the evolution of CD8+ T cell memory in vivo. Eur. J. Immunol. *28*, 4382–4390.

Clements, C.S., Dunstone, M.A., Macdonald, W.A., McCluskey, J., and Rossjohn, J. (2006). Specificity on a knife-edge: The alphabeta T cell receptor. Curr. Opin. Struct. Biol. *16*, 787–795.

Clements, C.S., Kjer-Nielsen, L., MacDonald, W.A., Brooks, A.G., Purcell, A.W., McCluskey, J., and Rossjohn, J. (2002). The production, purification and crystallization of a soluble heterodimeric form of a highly selected T-cell receptor in its unliganded and liganded state. Acta Crystallogr. D Biol. Crystallogr. *58*, 2131–2134.

Colf, L.A., Bankovich, A.J., Hanick, N.A., Bowerman, N.A., Jones, L.L., Kranz, D.M., and Garcia, K.C. (2007). How a single T cell receptor recognizes both self and foreign MHC. Cell *129*, 135–146.

Dai, S., Huseby, E.S., Rubtsova, K., Scott-Browne, J., Crawford, F., Macdonald, W.A., Marrack, P., and Kappler, J.W. (2008). Crossreactive T cells spotlight the germline rules for [alpha][beta] T cell-receptor interactions with MHC molecules. Immunity *28*, 324–334.

DeLano, W.L. (2002). The PyMOL Molecular Graphics System. http://www.pymol.org.

Deng, L., and Mariuzza, R.A. (2007). Recognition of self-peptide-MHC complexes by autoimmune T-cell receptors. Trends Biochem. Sci. *32*, 500–508.

Ding, Y.H., Smith, K.J., Garboczi, D.N., Utz, U., Biddison, W.E., and Wiley, D.C. (1998). Two human T cell receptors bind in a similar diagonal mode to the HLA-A2/Tax peptide complex using different TCR amino acids. Immunity *8*, 403–411.

Ely, L.K., Beddoe, T., Clements, C.S., Matthews, J.M., Purcell, A.W., Kjer-Nielsen, L., McCluskey, J., and Rossjohn, J. (2006). Disparate thermodynamics governing T cell receptor-MHC-I interactions implicate extrinsic factors in guiding MHC restriction. Proc. Natl. Acad. Sci. USA *103*, 6641–6646.

Ely, L.K., Green, K.J., Beddoe, T., Clements, C.S., Miles, J.J., Bottomley, S.P., Zernich, D., Kjer-Nielsen, L., Purcell, A.W., McCluskey, J., et al. (2005). Antagonism of antiviral and allogeneic activity of a human public CTL clonotype by a single altered peptide ligand: implications for allograft rejection. J. Immunol. *174*, 5593–5601.

Evans, P. (2006). Scaling and assessment of data quality. Acta Crystallogr. D Biol. Crystallogr. *62*, 72–82.

Feng, D., Bond, C.J., Ely, L.K., Maynard, J., and Garcia, K.C. (2007). Structural evidence for a germline-encoded T cell receptor-major histocompatibility complex interaction 'codon'. Nat. Immunol. *8*, 975–983.

Garboczi, D.N., Ghosh, P., Utz, U., Fan, Q.R., Biddison, W.E., and Wiley, D.C. (1996). Structure of the complex between human T-cell receptor, viral peptide and HLA-A2. Nature *384*, 134–141.

Garcia, K.C., Degano, M., Pease, L.R., Huang, M., Peterson, P.A., Teyton, L., and Wilson, I.A. (1998). Structural basis of plasticity in T cell receptor recognition of a self peptide-MHC antigen. Science *279*, 1166–1172.

Godfrey, D.I., Rossjohn, J., and McCluskey, J. (2008). The fidelity, occasional promiscuity, and versatility of T cell receptor recognition. Immunity *28*, 304–314.

Gras, S., Kjer-Nielsen, L., Burrows, S.R., McCluskey, J., and Rossjohn, J. (2008). T-cell receptor bias and immunity. Curr. Opin. Immunol. *20*, 119–125.

Hahn, M., Nicholson, M.J., Pyrdol, J., and Wucherpfennig, K.W. (2005). Unconventional topology of self peptide-major histocompatibility complex binding by a human autoimmune T cell receptor. Nat. Immunol. *6*, 490–496.

Hogquist, K.A., Gavin, M.A., and Bevan, M.J. (1993). Positive selection of CD8+ T cells induced by major histocompatibility complex binding peptides in fetal thymic organ culture. J. Exp. Med. *177*, 1469–1473.

Jameson, S.C., Hogquist, K.A., and Bevan, M.J. (1995). Positive selection of thymocytes. Annu. Rev. Immunol. *13*, 93–126.

Jones, T.A., Zou, J.Y., Cowan, S.W., and Kjeldgaard, M. (1991). Improved methods for building protein models in electron density maps and the location of errors in these models. Acta Crystallogr. A *47*, 110–119.

Kjer-Nielsen, L., Clements, C.S., Brooks, A.G., Purcell, A.W., Fontes, M.R., McCluskey, J., and Rossjohn, J. (2002a). The structure of HLA-B8 complexed to an immunodominant viral determinant: peptide-induced conformational changes and a mode of MHC class I dimerization. J. Immunol. *169*, 5153–5160.

Kjer-Nielsen, L., Clements, C.S., Brooks, A.G., Purcell, A.W., McCluskey, J., and Rossjohn, J. (2002b). The 1.5 A crystal structure of a highly selected antiviral T cell receptor provides evidence for a structural basis of immunodominance. Structure *10*, 1521–1532.

Kjer-Nielsen, L., Clements, C.S., Purcell, A.W., Brooks, A.G., Whisstock, J.C., Burrows, S.R., McCluskey, J., and Rossjohn, J. (2003). A structural basis for the selection of dominant alphabeta T cell receptors in antiviral immunity. Immunity *18*, 53–64.

Lawrence, M.C., and Colman, P.M. (1993). Shape complementarity at protein/protein interfaces. J. Mol. Biol. *234*, 946–950.

Lefranc, M.P., Giudicelli, V., Kaas, Q., Duprat, E., Jabado-Michaloud, J., Scaviner, D., Ginestoux, C., Clement, O., Chaume, D., and Lefranc, G. (2005). IMGT, the international ImMunoGeneTics information system. Nucleic Acids Res. *33*, D593–D597.

Leslie, A.G.W. (1992). Recent changes to the MOSFLM package for processing film and image plate data. Joint CCP4 and ESF-EAMCB Newsletter on Protein Crystallography, *26*.

Li, Y., Huang, Y., Lue, J., Quandt, J.A., Martin, R., and Mariuzza, R.A. (2005). Structure of a human autoimmune TCR bound to a myelin basic protein self-peptide and a multiple sclerosis-associated MHC class II molecule. EMBO J. *24*, 2968–2979.

Macdonald, W.A., Purcell, A.W., Mifsud, N.A., Ely, L.K., Williams, D.S., Chang, L., Gorman, J.J., Clements, C.S., Kjer-Nielsen, L., Koelle, D.M., et al. (2003). A naturally selected dimorphism within the HLA-B44 supertype alters class I structure, peptide repertoire, and T cell recognition. J. Exp. Med. *198*, 679–691.

Marsh, S.G., Albert, E.D., Bodmer, W.F., Bontrop, R.E., Dupont, B., Erlich, H.A., Geraghty, D.E., Hansen, J.A., Hurley, C.K., Mach, B., et al. (2005). Nomenclature for factors of the HLA system, 2004. Tissue Antigens *65*, 301–369.

Maynard, J., Petersson, K., Wilson, D.H., Adams, E.J., Blondelle, S.E., Boulanger, M.J., Wilson, D.B., and Garcia, K.C. (2005). Structure of an autoimmune T cell receptor complexed with class II peptide-MHC: insights into MHC bias and antigen specificity. Immunity *22*, 81–92.

McCluskey, J., Boyd, L., Foo, M., Forman, J., Margulies, D.H., and Bluestone, J.A. (1986). Analysis of hybrid H-2D and L antigens with reciprocally mismatched aminoterminal domains: functional T cell recognition requires preservation of fine structural determinants. J. Immunol. *137*, 3881–3890.

Messaoudi, I., Guevara Patino, J.A., Dyall, R., LeMaoult, J., and Nikolich-Zugich, J. (2002). Direct link between mhc polymorphism, T cell avidity, and diversity in immune defense. Science *298*, 1797–1800.

Nicholson, M.J., Hahn, M., and Wucherpfennig, K.W. (2005). Unusual features of self-peptide/MHC binding by autoimmune T cell receptors. Immunity *23*, 351–360.

Read, R.J. (2001). Pushing the boundaries of molecular replacement with maximum likelihood. Acta Crystallogr. D Biol. Crystallogr. *57*, 1373–1382.

Reid, S.W., McAdam, S., Smith, K.J., Klenerman, P., O'Callaghan, C.A., Harlos, K., Jakobsen, B.K., McMichael, A.J., Bell, J.I., Stuart, D.I., and Jones, E.Y. (1996a). Antagonist HIV-1 Gag peptides induce structural changes in HLA B8. J. Exp. Med. *184*, 2279–2286.

Reid, S.W., Smith, K.J., Jakobsen, B.K., O'Callaghan, C.A., Reyburn, H., Harlos, K., Stuart, D.I., McMichael, A.J., Bell, J.I., and Jones, E.Y. (1996b). Production and crystallization of MHC class I B allele single peptide complexes. FEBS Lett. *383*, 119–123.

Reiser, J.B., Darnault, C., Gregoire, C., Mosser, T., Mazza, G., Kearney, A., van der Merwe, P.A., Fontecilla-Camps, J.C., Housset, D., and Malissen, B. (2003). CDR3 loop flexibility contributes to the degeneracy of TCR recognition. Nat. Immunol. *4*, 241–247.

Reiser, J.B., Gregoire, C., Darnault, C., Mosser, T., Guimezanes, A., Schmitt-Verhulst, A.M., Fontecilla-Camps, J.C., Mazza, G., Malissen, B., and Housset, D. (2002). A T cell receptor CDR3beta loop undergoes conformational changes of unprecedented magnitude upon binding to a peptide/MHC class I complex. Immunity *16*, 345–354.

Rossjohn, J., and McCluskey, J. (2007). How a home-grown T cell receptor interacts with a foreign landscape. Cell *129*, 19–20.

Rudolph, M.G., Stanfield, R.L., and Wilson, I.A. (2006). How TCRs bind MHCs, peptides, and coreceptors. Annu. Rev. Immunol. *24*, 419–466.

Turner, S.J., Doherty, P.C., McCluskey, J., and Rossjohn, J. (2006). Structural determinants of T-cell receptor bias in immunity. Nat. Rev. Immunol. *6*, 883–894.

Tynan, F.E., Burrows, S.R., Buckle, A.M., Clements, C.S., Borg, N.A., Miles, J.J., Beddoe, T., Whisstock, J.C., Wilce, M.C., Silins, S.L., et al. (2005). T cell receptor recognition of a 'super-bulged' major histocompatability complex class I-bound peptide. Nat. Immunol. *6*, 1114–1122.

Tynan, F.E., Reid, H.H., Kjer-Nielsen, L., Miles, J.J., Wilce, M.C., Kostenko, L., Borg, N.A., Williamson, N.A., Beddoe, T., Purcell, A.W., et al. (2007). A T cell receptor flattens a bulged antigenic peptide presented by a major histocompatibility complex class I molecule. Nat. Immunol. *8*, 268–276.

Zinkernagel, R.M., and Doherty, P.C. (1974). Immunological surveillance against altered self components by sensitised T lymphocytes in lymphocytic choriomeningitis. Nature *251*, 547–548.